Research Journal of Applied Sciences, Engineering and Technology 5(3): 962-969, 2013
DOI:10.19026/rjaset.5.5047
ISSN: 2040-7459; E-ISSN: 2040-7467

Submitted: June 22, 2012 Accepted: July 23, 2012 Published: January 21, 2013

Research Article

A MEMS Flow Sensor for Self-adjusted Precise Non-Contact Liquid Dispensing

[1,2]Liu Yaxin, [1]Zhong Ming and [1]Yao Yufeng
[1]State Key Laboratory of Robotics and System, Harbin Institute of Technology, Harbin 150001, P.R. China
[2]State Key Laboratory for Manufacturing Systems Engineering, Xi'an Jiaotong University, Xi'an 710049, P.R. China

Abstract: A MEMS flow sensor was proposed to enhance the reliability and accuracy of liquid dispensing system. Benefiting from the feedback of sensor information, the system can self-adjust the open time of the solenoid vale to accurately dispensing desired reagent volume without pre-calibration. This study focuses on the design, fabrication and application of this flow sensor. Firstly, the design, fabrication and characteristics of the MEMS flow sensor based on the measurement of the pressure difference across a flow channel are presented. Secondly, the liquid dispensing system in which the flow sensor is integrated will be introduced. A novel closed-loop control strategy is proposed to calculate valve open-time for each dispensing cycle. Finally, experiments results are presented with different dispensing volumes, Coefficient of Variance (CV) has been shown to be below 3%. It indicates that integration of the MEMS flow sensor and using of a compound intelligent control strategy make the system immune to liquid viscosity, pressure fluctuation and some other disturbances.

Keywords: Flow sensor, liquid dispensing, MEMS

INTRODUCTION

During the past decades, volume transfers of liquids in the submicroliter range have become an important feature of liquid-handling robotic instruments (Peddi *et al*., 2007; Stock *et al*., 2005). In order to dispense smaller volumes than that can be dispensed by hand with more accuracy, higher speed and better reproducibility, many automated liquid dispensing technologies have been developed in academic and commercial applications (Liu *et al*., 2007; Samel *et al*., 2008; Hazes and Price, 2005; Englmann *et al*., 2007; Ahmed and Jones, 2006; Bergkvist *et al*., 2005). While, in some application conditions, such as protein crystallization, drug discovery and medical diagnostics, many reagents with different viscosities needed to be dispensed during one screening experiment (Hui and Edwards, 2003; Robert *et al*., 2003; Podolak, 2010). Most of the commercial automated liquid dispensing systems could not adjust system parameters automatically. The dispensing device operating under identical conditions will dispense more liquid with lower viscosity and less liquid with higher viscosity. So, dispense volume errors are introduced when liquids of different viscosities are handled simultaneously.

In order to resolve this problem, a MEMS flow sensor based on the measurements of pressure difference across a micro flow channel was proposed to use in a high throughput non-contact dispensing system. The properly designed dimensions make it adapt to the static and dynamic requirements of the non-contact liquid dispensing process and suitable for high-speed flow sensing in the high-throughput liquid dispensing system. Otherwise, the electrical contacts of the flow sensor are fully galvanic insulated from the fluid, which is suitable for medicine dosing or some chemical analysis application. Besides, there are no energy injections in the liquid when the sensor works. So, heating up of the fluid is negligible, which is an important issue for dispensing temperature sensitive materials.

With feedback information from the flow sensor, dispensing system could self-adjust the open time of solenoid vale and the system pressure to dispense desired volume reagents with a large range of viscosities. Besides, air bubbles or nozzle clogs can be detected in real time. This study focuses on the design, fabrication and application of this flow sensor.

METHODOLOGY

Design and analyses:

Sensor principle: Functional layout of the sensor is shown in Fig. 1. It consists of 2 piezo-resistive sensor dies where the micro-machined channel embedded. By use of anodic bonding process, glass wafer is mounted

Corresponding Author: Zhong Ming, State Key Laboratory of Robotics and System, Harbin Institute of Technology, Harbin 150001, P.R. China

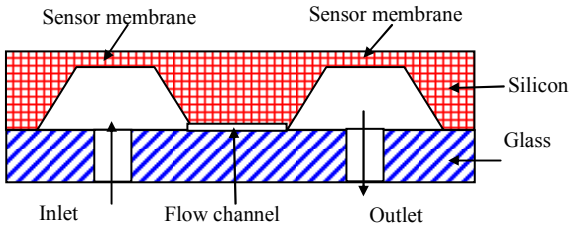

Fig. 1: The schematic structure of the sensor-chip

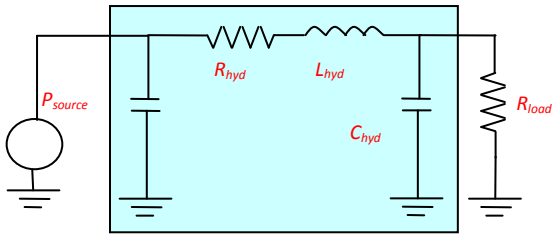

Fig. 2: Electric analogy of the flow sensor

on the silicon wafer. The pressure drop caused by liquid flowing across the micro-machined channel at low Reynolds numbers is expressed as (1):

$$\Delta P = Q_V \times \frac{C \mu L}{2AD_h^2} \quad (1)$$

where,
ΔP : Pressure drop (Pa)
Qv : Volumetric flow rate (m^3/s)
C : Dimensionless friction factor
μ : Fluid dynamic viscosity (Pa. s)
L : Channel length (m)
A : Channel cross section (m^2)
Dh : Equivalent hydraulic diameter (m), equal to 4 A/wetted

It shows that we can read the flow rate from the pressure drop. In the liquid dispensing system, the sensor was located between the pressure source and the solenoid valve where only the system fluid (de-ionized water) flows through, so its sensitivity is determined by physical dimensions of the flow channel. And the pressure can be read from the piezo-resistives on silicon membranes.

Dimensions design: Dimensions of silicon membranes and micro-flow channel are the key factors affecting the characteristic of flow sensor.

When design the silicon membranes, the following formulas should be considered. The membranes should not be broken at maximum 15 psi pressure of the liquid dispensing system. And besides, deflection of the membrane should be as small as possible to ensure elastic deformation. Generally, if the max center deflection of the membrane is smaller than half of the membrane thickness, the deformation can be considered as elastic deformation. The piezo-resistors are placed in a Wheatstone bridge on the membranes and output of the Wheatstone bridge should be large enough to enhance the sensitivity.

As square diaphragm is considered, the center deflection (w_{max}) and the stress ($|\sigma|_{max}$) near the edge could be estimated by (2) and (3). Output of the Wheatstone bridge (u_i) can be given by (4):

$$w_{\max} \approx 0.0151 \frac{pa^4}{Eh^3}(1-\nu^2) \quad (2)$$

$$|\sigma|_{\max} \approx 0.3078 \frac{pa^2}{h^2} \quad (3)$$

$$u_i = u(\Delta R / R) = uK\sigma \quad (4)$$

where,
P : The pressure on the membrane (Pa)
E : The elasticity modulus of silicon (Pa)
v : The Poisson's ratio
a : The width of the membrane (m)
h : The thickness of the membrane (m)
u : The bridge voltage (V)
K : The Piezo-resistive coefficient

Based on the formulas presented: $w_{max}<0.5h$; $|\sigma|_{max}<80$ MPa; $ui/u>1$ mV/V, the size of membrane should be limited by formula (5):

$$21.9677<a/h<50.98 \quad (5)$$

Thus, the prototypes of the sensor were designed, which consist of square silicon membranes of about 50 μm and a length and width of 2000 μm. The simulation results of single membrane by ANSYS show that the maximum stress at 15 psi is 2.5E7 Pa and the maximum deflection is 1.3 μm. The full scale stress and deflection are all less than limited values.

Micro-flow channel is the other key factor affecting the characteristic of the flow sensor. Varying the channel dimensions makes it possible to adapt the sensor for a specific flow range. In our liquid dispensing system, the required liquid flow rate is about several 10 μL/s. So, the channel length is designed as 2005 μm, the depth is 30 μm and the width is 30 μm. Pressure drop across the micro channels simulated by CFD software (Fluent) is less than 5 psi.

Dynamic analyses: In the liquid dispensing system, the flow sensor is operated in the dispensing system with fast fluid speeds, so it is important to know the dynamic behavior to predict the time dependent signal from the flow and pressure. A lumped electric element analogy of the flow sensor was used to estimate the working range as shown in Fig. 2.

Besides the computed hydraulic resistance of the channel, the sensor also consists of hydraulic capacities C_{hyd} and inertance L_{hyd} (Kovacs, 1998). The transfer function of the LRC circuit and the resonance frequency f_{hyd} of it are expressed as (6) and (7):

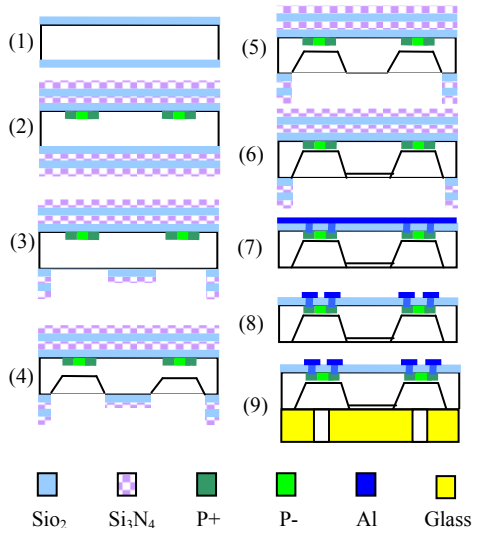

Fig. 3: Process sequences of the pressure/flow-sensor chip

$$G_{hyd} = \frac{1}{1 + j\omega R_{hyd} C_{hyd} - \omega^2 L_{hyd} C_{hyd}} \quad (6)$$

$$f_{hyd} = \frac{1}{2\pi\sqrt{L_{hyd} C_{hyd}}} \quad (7)$$

It can be concluded that it is possible to increase f_{hyd} by reducing C_{hyd} and L_{hyd} to obtain a higher dynamic range. Due to the square membrane deflection under a pressure load, liquid can be accumulated. The hydraulic capacity of the sensor is expressed in (8). The iterance of the sensor is caused by the acceleration of liquid mass in the sensor and defined by (9):

$$C_{hyd} = 0.28\frac{(a/2)^6}{Eh^3}(1-\nu^2) \quad (8)$$

$$L_{hyd} = \rho l / A \quad (9)$$

where,
L : Channel length (m)
A : Channel cross section (m^2)
D_h : Equivalent hydraulic diameter (m)
E : Modulus of elasticity (Pa)
v : Poisson constant
ρ : Density (kg/m^3)
a : Membrane width (m)
h : Membrane thickness (m)

It can be seen that the dynamic behavior has relations with the stiffness of the membrane and the dimension of the channel. When the channel length is designed as 2005 μm and the depth is 30 μm. For the 2000 μm width channel, the resistance for water becomes 3.36×10^{11} Ns/m^5 with an inertance of 3.2×10^7 kg/m^4. The resonance frequency is 7019 Hz and the sensor can be used dynamically with a fluid frequency up to 1 kHz.

Fabrications and packaging: We started the fabrication process in 400 μm-thick (100) oriented silicon wafers. The detailed process flow is described as shown in Fig. 3:

- The sensor was fabricated by using a 4-inch (100) orientation double polished silicon wafer with a thickness of 400 μm. And 0.5 μm thick thermal oxide layers are grown on both sides of the wafer, which is used as the protection layer for the boron infusion.
- The piezoresistive Wheatstone bridge regions are patterned by photolithography on the front side of the wafer and buffered HF etching. Then the piezoresistors were formed by boron ion implantation in the regions. A drive-in process was done to activate boron ions.
- The membranes and channel are anisotropic etched using double mask technique. The SiO_2 is deposited on the silicon substrate followed by a deposition of LPCVD Si_3N_4 on the oxide layer. Then the same deposition process is performed again. The membranes were patterned by photolithography on the backside of the wafer. The double SiO_2 and Si_3N_4 masks on membranes areas were etched and the single SiO_2 and Si_3N_4 masks on channel areas were etched away.

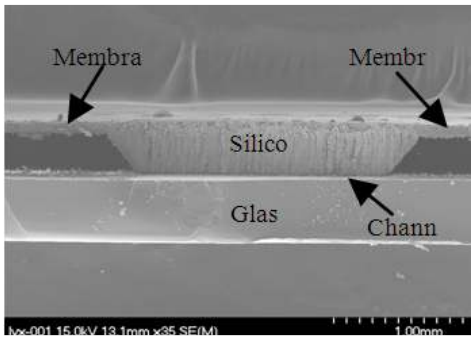

(a)

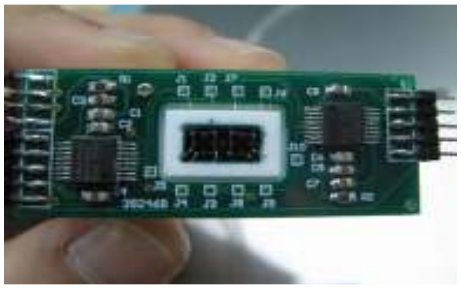

(b)

Fig. 4: Cross section view and the photo of the sensor packaging

- Backside etching process was performed in KOH to form membranes.
- In order to reveal the channel pattern on the silicon substrate, the masks SiO_2 and Si_3N_4 were etched once more.
- The channel and the membranes were etched in KOH again.
- The contact holes are patterned by photolithography and opened by wet etching in buffered HF solution. Then 0.8 μm-thick aluminum is sputtered.
- Aluminum wires and bonding pads were formed by vacuum evaporation, photolithography and etching processes.
- The glass wafer with 1.8 mm holes is mounted on the silicon wafer by anodic bonding process. The holes on the glass are created using ultrasonic machining process.

A SEM picture of cross-section of the sensor chip is shown in Fig. 4a.

The finished sensor chip is mounted on a ceramic substrate on which compensating electrical circuits and fluidic connections are all placed. Outputs of sensor chip are magnified and calibrated by 2 signal-conditioner ICs---Max1452. Figure 4b shows the photo of the packaging configuration. Before the sensor is devoted to wok, electrical circuit module should be connected to the communication module for calibration. In the next part, the calibration process will be explained in detail.

Characteristics: Figure 5a shows the schematic of experimental set up for pressure-voltage calibration for the MEMS flow sensor. It mainly consists of computer, pressure regulator, pressured fluid bottle, flow sensor, solenoid valve and valve controller. Computer communicates with the pressure regulator to output a settled pressure. The pressured gas connects with one port of a 2 L solvent bottle capped with a 2-port fittings cap. The other port connects to flow sensor to supply pressured water. The goal of such a system is to supply a controlled constant pressure. First of all, make sure that electrical circuit module of the sensor is connected to the communication module which is connected to PC; at this time, max1452 works in digital mode. Due to the desired sensor output for each pressure and the measured values, the computer will calculate and write the calculated compensation coefficients into the EEEPROM of max1452. And then remove communication module and leave the electrical circuit module work alone; at this time, the max1452 works in analog mode and the voltage output of pressure sensor has been calibrated as desired values. Figure 5b shows the calibrated signal output for different system pressure conditions. The non-linearity of pressure sensor is 0.29%.

The flow-voltage calibration system mainly consists of computer, syringe pump, flow sensor, solenoid vale and valve controller as shown in Fig. 6a. The syringe pump can supply 40 kinds of flow rates

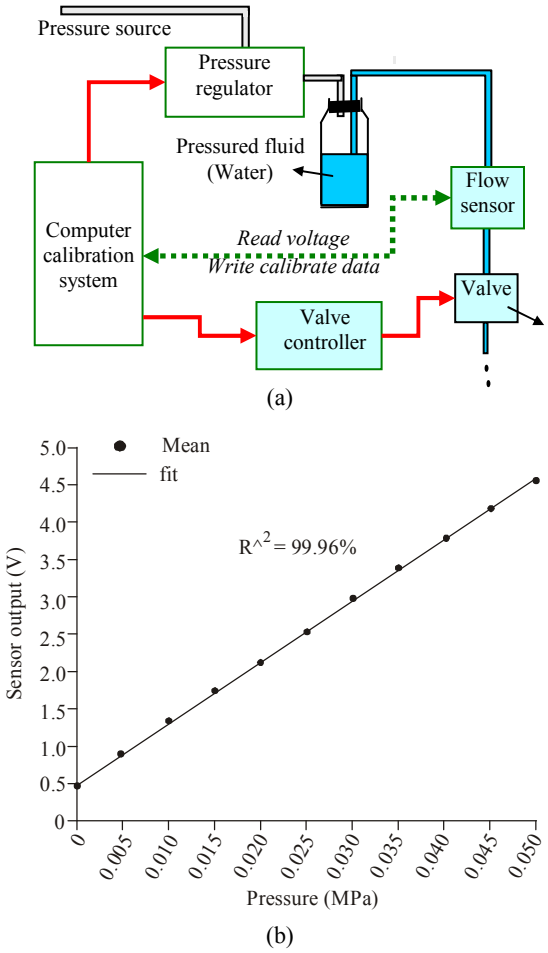

Fig. 5: (a) The schematic of experimental set up for pressure-voltage calibration, (b) Measured output voltages for different pressures, the 'goodness of fit' statistics (R^2) is 99.96%

range from 0.4167 μL/s up to 300 uL/s. In each flow condition, the corresponding average output voltage was recorded. The output voltage differences for different flow rate are shown in Fig. 6b. The sensitivity of the calibrated sensor is 31 mV/ (μL/s) and the non-linearity is 0.51%.

Finally, flow rate (given by syringe pump, 25 μL/s) was measured with the MEMS flow sensor and electronic balance separately for 21 times and the test results show that the measurement reproducibility is below 0.67%. And the sensor response time is shorter than 1.5 ms.

APPLICATIONS

The liquid dispensing system: The schematic of the non-contact liquid dispensing system developed by our team is shown in Fig. 7. The dispensing system consists of syringe pump, syringe valve, pressurized regent bottle, pressure regulator, micro solenoid valves and sensors, etc.

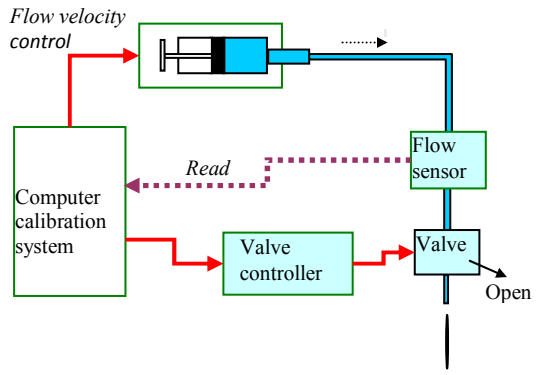

(a)

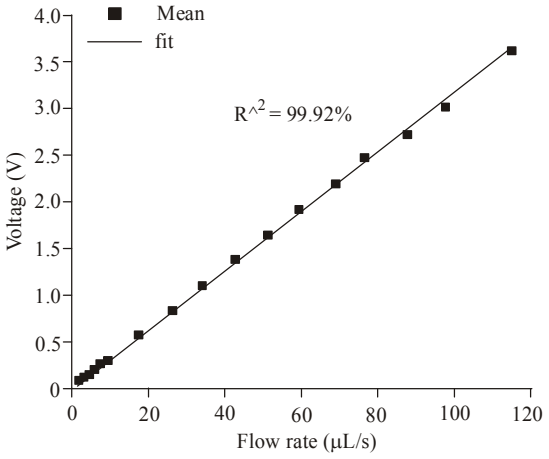

(b)

Fig. 6: (a)The schematic of experimental set up for flow-voltage drop calibration, (b) Sensor voltage output for different flow rate, the 'goodness of fit' statistics (R^2) is 99.92%

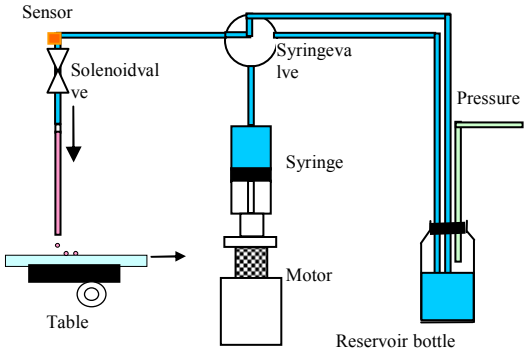

Fig. 7: Schematic of solenoid-based non-contact liquid handling

Using the flow sensor, the dispensing system could adjust open-time of the solenoid vale and system pressure automatically to dispense desired volume reagents with a large range of viscosities and detect air bubbles or nozzle clogs in real time. The photo of the dispensing system is shown in Fig. 8.

Fig. 8: The photo of the dispensing system

Self-adjusted feedback control method: The schematic of the compound intelligent control strategy used in the liquid dispensing system is shown in Fig. 9.

In each dispensing cycle T, The feedback flow velocity starts to be integrated at the moment the valve is open. The actual dispensed volume V_T during each cycle and the dispensed volume V_t during open-time can be calculated via real-time flow pulse integration. In the next dispensing cycle, if the volume error between V_0 and V_T, namely E, is larger than critical value m, the new valve open-time will be set via "RV Compensation" strategy; otherwise it will be set by a fuzzy control strategy.

The mentioned "RV Compensation" strategy mainly considers effect of residual volume, which is similar to that proposed by Cars ten (Haber *et al*., 2005). For example, the demanded volume is V_0 and the valve will opened for a timed interval until the V_0 is dispensed at a given system pressure. But when the valve is closed, the flow rate will be not immediately reset to zero, which leads to that redundant volume dV is dispensed and that the overall dispensed volume is V_0+dV. So, in the next dispensing cycle, the residual volume will be taken into account and the desired volume is considered as V_0-dV. At the dispense trigger, the system begins to integrate the flow pulse and then closes the valve in the exact moment when the new set point has been reached, thus dispensing accurately the requested volume. It can be seen that the minimum controlled dispensed volume is determined by the residuum volume. When the residual volume exceeds the requested volume, the system no longer is capable to deliver the correct volume. Especially in the non-contact dispensing process, the flow rate is higher than 20 μL/s normally, which results in that approximately 200-250 nL residual volume is dispensed after valve is closed. So it is difficult to dispense correct volume larger than 200 nL only using "residual volume compensation" strategy in this system. Figure 10 shows the actual dispensed volumes for initial 50 cycles with the conventional RV compensation strategy only.

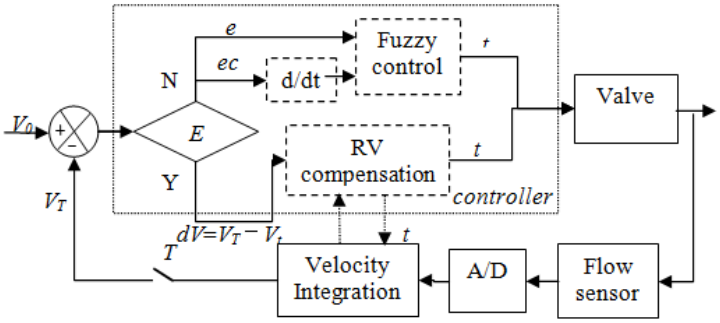

Fig. 9: The schematic of the compound intelligent control strategy

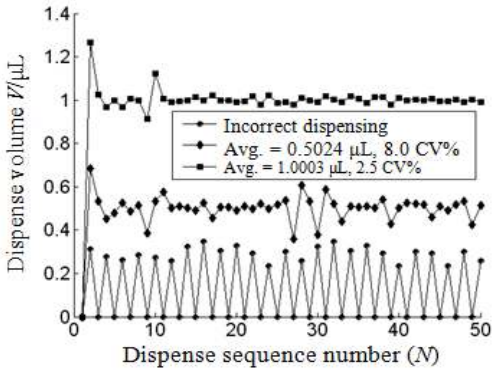

Fig. 10: The dispensed volume in each cycle with only RV compensation strategy

It is obvious that precision deteriorates as the dispensed volume is reduced. When the desired volume is reduced to 0.1 μL, the system cannot work correctly only with the conventional RV compensation strategy.

Besides, the viscous reagent exist in the pipe reduces gradually during dispensing process, which leads to that the identical viscosity decrease gently. The system pressure and viscosity fluctuations may all affect dispensing precision.

So a fuzzy controller is introduced to dispense smaller desired volume. For fuzzy control, the minimum controlled dispensed volume lie on the response time of the valve. If the calculated open-time is smaller than the response time of the valve, the valve will not open normally. Using this method, the minimum controllable dispensed volume depends on the valve response time rather than the residual volume and the system will not run away until the calculated valve open time is smaller than the valve response time. So the system can dispense smaller volume with fuzzy control strategy. Figure 11a shows the actual dispensed volumes in initial 50 cycles with fuzzy control strategy only. It can be seen that the precision does not get worse with reduction of dispensing volume and the system can also dispense exact volume despite the small desired volume of 0.1 μL. However, this method

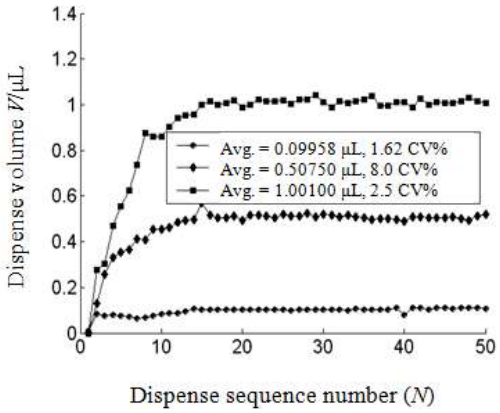

(a)

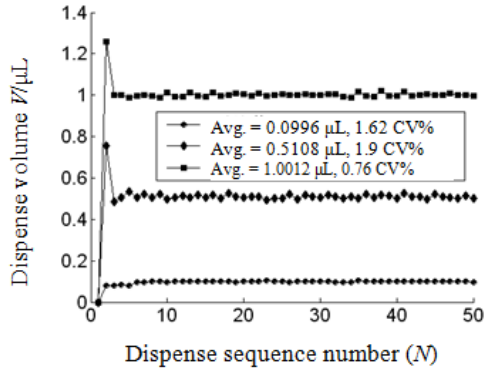

(b)

Fig. 11: Dispensed volume for each cycle with different control strategies, desired volume and reagent. (a) fuzzy method only (b) intelligent compound control strategy

still has shortcomings; it must pre-dispense several times to achieve the desired volume.

Therefore, an intelligent compound control strategy which combines residual volume compensation method and fuzzy control strategy is proposed, as shown in Fig. 11b.

Table 1: Reproducibility of the dispenses

	Reproducibility (CV%)			
Reagent	0.1 μL	0.5 μL	1 μL	5 μL
Water	1.62	1.40	0.76	0.40
10% glycerol	1.03	1.80	2.00	0.50
20% glycerol	2.60	2.00	2.30	0.54
30% glycerol	1.90	3.20	2.20	0.59
40% glycerol	2.35	2.00	1.39	1.96
50% glycerol	3.30	3.70	1.97	1.20

Table 2: Reproducibility for dispensing 5% glucose, alcohol, 2.5% PEG, hepes, Tris-Hcl, lymphocyte separation medium and DMSO

	100 nL		300 nL		500 nL		1 μL		5 μL	
Reagent	CV (%)	Avg. (nL)	CV (%)	Avg. (nL)	CV (%)	Avg. (nL)	CV (%)	Avg. (μL)	CV (%)	Avg. (μL)
5% glucose	0.89	101	0.66	298	0.31	499	0.41	0.995	0.79	5.060
Alcohol	1.80	98	2.95	304	1.98	505	2.83	1.020	0.20	505
2.5%PEG	2.80	107	0.45	307	0.30	500	0.76	1.006	0.56	5.020
Hepes buffer	3.20	102	0.98	295	1.50	498	0.24	1.009	0.78	5.003
Tris-Hcl	1.27	104	0.965	304	0.83	503	1.48	1.007	0.79	5.047
Lymphocyte separation medium	2.70	105	2.680	303	1.19	504	0.93	1.010	0.57	5.060
DMSO	2.85	105	1.98	302	1.43	507	1.48	101	0.63	5.060

It can be seen that by use of the intelligent compound control strategy, the system can not only dispense smaller volumes, but also dispense volumes close to the desired volume in the first cycle.

The novel intelligent control strategy combines the advantages of residual volume compensation method with the robustness of fuzzy logic controller. Using this method, the system could find appropriate valve open-time through only one pre-dispensing cycle without manual calibration and could constantly monitor and correct the dispense process to make this system immune to sample viscosity, pressure fluctuation and some other disturbances. Moreover, with the real-time information from the flow sensor, air bubbles or nozzle clogs can be diagnosed with feedback information.

DISPENSING EXPERIMENTS AND RESULTS

Finally, dispensing experiments were carried out with different volumes and reagents in 96-well plate. The experiment reagents were water, 10, 20, 30, 40 and 50% glycerol, respectively. For each reagent, the dispensing precision at 0.1, 0.5, 1 and 5 μL were tested and recorded, as shown in Table 1. The repetitive precision of the dispense system was evaluated by the Coefficient of Variance (CV %) that is calculated as follows:

$$CV\% = \frac{\sqrt{\frac{(\bar{X} - X)^2}{n-1}}}{\bar{X}} 100\% \quad (10)$$

where, $\bar{X}$ is average value; X is actual value; n is the number of measurements. It shows that coefficient of variance has been shown to be below 3% at μL and approach 4% at 100 nL.

Furthermore, when the reagents are 5% glucose solution, Alcohol, 2.5% PEG, Hepes buffer, Tris-Hcl, lymphocyte separation medium and DMSO solution, the dispensing precision at 0, 0.5, 1 and 5 μL were also tested and recorded, as shown in Table 2. It can be seen that dispensing precision didn't get worse when dispense conditions change and dispensing reproducibly is below 3%.

CONCLUSION

A flow sensor based on the measurement of pressure drop across a micro-channel is developed to use in the liquid dispensing system. In this study, the model, design, fabrication, packaging and characterization of differential pressure flow sensor were presented. The sensor's low dead volume, low power consuming, high speed, resolution and accuracy make it suitable for using in high throughput liquid dispensing system. Advanced intelligent compound fuzzy control strategy is introduced in detail. Dispensing results show that the system can achieve better dispensing performance by use of a compound intelligent fuzzy control strategy. Integration of the custom high-speed MEMS flow sensor and use of the compound intelligent control strategy make it possible to self-adjust the open time of the solenoid valve for dispensing desired volume reagents accurately with a large range of viscosities. Furthermore, it could constantly monitor and correct the dispensing process to make this system immune to sample viscosity, pressure fluctuation and some other disturbances. Finally, the dispensing experiment results show that the Coefficient of Variance (CV) for liquid dispensing is below 3% at 1 μL and below 4% at 100 nL.

ACKNOWLEDGMENT

This study was supported by National Natural Science Foundation of China (No. 51105116), 863 Program of China (2011AA040406), State Key Laboratory of Robotics and System (HIT, SKLRS-2010-MS-20), State Key Laboratory for Manufacturing Systems Engineering (Xi'an Jiao tong University, 2011004) and Natural Scientific Research Innovation Foundation in Harbin Institute of Technology (HIT. NSRIF.201005).

REFERENCES

Ahmed, R. and T.B. Jones, 2006. Dispensing picoliter droplets on substrates using dielectrophoresis. J. Electrostat., 64(7-9): 543-549.

Bergkvist, J., T. Lilliehorn, J. Nilsson, S. Johansson and T. Laurell, 2005. Miniaturized flowthrough microdis-penser with piezoceramic tripod actuation. J. Microelectromech. S., 14(1): 134-140.

Englmann, M., A. Fekete, I. Gebefügi and P. Schmitt-Kopplin, 2007. The dosage of small volumes for chromatographic quantifications using a drop-on-demand dispenser system. Anal. Bioanaly-tical Chem., v 388(5-6): 1109-1116.

Haber, C., M. Boillat and B.V.D. Schoot, 2005. Precise nanoliter fluid handling system with integrated high-speed flow sensor. ASSAY Drug Dev. Technol., 2: 203-212.

Hazes, B. and L. Price, 2005. A nanovolume crystallization robot that creates its crystallization screens on-the-fly. Acta. Crystallographica Section D Biol. Crystallography, D61: 1165-1171.

Hui, R. and A. Edwards, 2003. High-throughput protein crystallization. J. Struct. Biol., 142: 154-161.

Kovacs, G.T.A., 1998. Micromachined Transducers Source-Book, 1998. McGraw-Hill Co. Inc., ISBN-10: 0072907223: ISBN-13: 978-0072907223.

Liu, Y.X., L.G. Chen, L.N. Sun and W.B. Rong, 2007. Automated submicroliter fluid dispensing technology for protein Crystallization. J. Bas. Sci. Eng., 15: 111-120.

Peddi, A., L. Muthusubramaniam, Y.F. Zheng, V. Cherezov, Y. Misquitta, *et al*., 2007. High-throughput automated system for crystallizing membrane proteins in lipidic mesophases. IEEE T. Autom. Sci. Eng., 4(2): 129-140.

Podolak, E., 2010. New cell printing approach enables precise design of complex 3-D tissue structures. Int. J. Life Sci. Methods, 48(2).

Robert, J.R., J. Collins A. Nancy and A. Fehrman, 2003. A deliberate approach to screening for initial crystalli-zation conditions of biological macromolecules. J. Struct. Biol., 142: 170-179.

Samel, B., N. Sandström, P. Griss and G. Stemme, 2008. Liquid Aspiration and Dispensing Based on an Expanding PDMS composite. J. Microelectro-mechanical Syst., 17(5): 1254-1262.

Stock, D., O. Perisic and J. Lowe, 2005. Robotic nanolitre protein crystallisation at the MRC Laboratory of Molecular Biology. Prog. Biophys. Mol. Bio., 88: 311-327.